Korean J. Chem. Eng., 37(3), 563-570 (2020)
DOI: 10.1007/s11814-019-0452-2

pISSN: 0256-1115
eISSN: 1975-7220

Fabrication methods of dry adhesive with various shaped microsuction cups

Myeongju Kang and Younghun Kim†

Department of Chemical Engineering, Kwangwoon University, 20 Kwangwoon-ro, Nowon-gu, Seoul 01897, Korea
(*Received 23 October 2019 • accepted 1 December 2019*)

Abstract−Bio-inspired micro- and nanostructures are emerging as novel dry adhesives owing to their high aspect ratio micropillar structure, resulting in collective van der Waals attraction between the adhesive and the substrate. Specifically, gecko-inspired structures exhibit great adhesive properties on smooth surfaces; however, the pull-off strength of micropillars in gecko-inspired surfaces can be decreased by applying a preloading force. Therefore, octopus suckers or suction cup-like structures have been considered as alternative microstructures providing high adhesion force. The fabrication of both microsuckers and micropillar structures is complicated and requires sophisticated control of the microstructure using photolithography and sequential polymer-based replica molding. Therefore, in this study, a fabrication method for octopus-like and suction cup-like micropatterns on polymer matrix is suggested by simple replica molding using a single master wafer. The relationship between the total adhesion force and the effective surface area of micropatterns was established and calculated by summing the preloading force, the suction force in the normal direction, and the shear force induced by van der Waals attraction. The results of adhesion force measurement and the repeatability test show that the micropatches with square microholes have high adhesion force (16 N/cm^2) and good repeatability of attachments/detachments over 100 cycles.

Keywords: Polydimethylsiloxane, Suction Cup, Dry Adhesive, Shear Stress

INTRODUCTION

Pressure-sensitive adhesives (PSA) are typically used as nonstructural self-adhesive tapes without the chemical reactions of epoxies in conventional adhesives [1]. For the short contact of PSA tapes on the target surfaces, the only interaction energy in the PSA adhesion results from van der Waals (vdW) forces [2]. The vdW forces generally increase with an increase in the contact area between the tape and the surface; thus, a hierarchical hairpin configuration with large contact area was suggested as a possible nanostructure to enhance the self-adhesion force. Due to the significant advances in the development of artificial tactile sensors and epidermal medical patches, research on elastomeric dry adhesives has intensified recently [3]. Specifically, gecko-inspired structures consisting of high aspect ratio nanopillars have been introduced for reversible attachment with collective vdW adhesion [4]. Mushroom-like micropillar structures also showed enhanced skin adhesive properties with an adhesion force of ~1.8 N/cm^2 [5,6], and wrinkled polymer sheets with built-in micropillars revealed relatively strong normal (~10 N/cm^2) and shear adhesion (~15 N/cm^2) [7]. An enhanced adhesive feature was revealed by decreasing the pillar diameter and increasing the number of pillars [8]. In addition, the fibrillary structure of gecko-inspired surfaces enables easy surface detachment along a preferential direction [9].

Another biomimetic strategy for dry adhesives is the fabrication of octopus-inspired microsuction cups. While dry adhesion by vdW forces performs well on smooth and clean surfaces, suction cups, exploiting the reduction of pressure to generate attachment forces, can be used on both smooth and partially rough surfaces [10]. Therefore, if the dry adhesives with microsuction cups have micropillar arrays as similar to gecko-adhesives, the pull-off strength could be decreased with increasing of the preloading force to generate the adhesive properties, owing to the lateral deformation of the adhesives' back film by the Poisson effect under excessive preload [11]. Therefore, an octopus-inspired architecture was suggested as an alternative configuration for dry adhesive films [12]. The dome-like protuberances in octopus-inspired microsuckers exhibited high adhesion performance in the normal direction due to enhanced suction effect supported by capillarity [13]. The total adhesion force of microsuckers is induced by both the elasto-capillary effects on the suction forces (negative pressure) and the dynamic contact effect on the vdW forces [14]. Therefore, compared with the micropillar structure, the microsucker structure can have higher adhesion properties.

Both the microsucker and micropillar structures have generally been fabricated on polymeric substrates such as polydimethylsiloxane (PDMS) by photolithography and subsequent molding. The entry barriers of studies on microsuckers adhesives fabrication using photolithography and replica molding are high due to the requirement of sophisticated control of the fine microstructure. Therefore, in this paper, a simple molding method of microsuction cup fabrication on PDMS is proposed by the depth and shape adjustment of holes in microsuction cups. The micropatterns of the holes are formed into triangular, square, hexagonal, and circular shapes. The adhesion force of PDMS with microsuction cups was measured using a pulley assembly enabling incremental loading. The micropatch fabricated with 7.5% curing agent on PDMS base exhibited high adhesion performance on a glass surface compared with that fabricated with 10% curing agent.

†To whom correspondence should be addressed.
E-mail: korea1@kw.ac.kr

EXPERIMENTAL

1. Fabrication of Suction Cup-like Micropatch

Dry adhesive micropatch with micron-size suction cups was fabricated by a series of surface micromachining steps and replica molding of PDMS. First, a master wafer (p-type, 100) with four differently shaped holes with depth of 12 μm was prepared by photolithography and subsequent deep reactive-ion etching (DRIE). Both the inter-distance between and the outer diameter of the microholes were fixed as 4 μm. Following the preparation of the master wafer, a PDMS replica was prepared by molding the PDMS prepolymer into the fabricated master. To fabricate the first PDMS replica, a 10 : 1 mixture of the PDMS prepolymer (Sylgard 184 A) and curing agent (Sylgard 184 B) was poured onto the master wafer. Following the removal of air bubbles formed during mixing, PDMS was cured onto the silicon master at 70 °C for 3 h. The PDMS replica (10%) was rapidly peeled off from the master wafer to obtain a cone-shaped mold on the wafer, as shown in Fig. 1. A PDMS mixture of 10.0 : 0.75 was then poured onto the master wafer with the cone-shaped mold. Following the curing, the PDMS replica (7.5%) was carefully removed from the master to obtain the suction cup-like microholes on the PDMS. While the first 10%-PDMS replica had a positive pattern with an octopus sucker shape, the second 7.5%-PDMS replica showed a negative pattern with suction cup-like microholes. The surface morphologies and depth profiles of the as-prepared micropatches were analyzed using atomic force microscopy (AFM, PSI-100, Park Systems). The surface area of microholes in PDMS was evaluated with a graphing and analysis software (OriginPro 2018).

2. Measurement of Adhesion Force

Adhesion measurements of the as-prepared 10%-PDMS replica with positive pattern and the 7.5%-PDMS replica with negative pattern were performed using a custom-made pulley arrangement for different loading. A flexible adhesive patch (with thickness of 1 mm of and unit area of 1 cm^2) was attached to a flat glass surface under a preload of 2.444 and 2.693 N/cm^2 for 10%- and 7.5%-PDMS, respectively. The hanging weight was increased until an adhesion failure occurred. This test was carried out 100 times for each sample under identical conditions. For comparison, the adhesion forces of the pristine PDMS sheets (10% and 7.5%) were also measured using the same procedure.

RESULTS AND DISCUSSION

Apparently, the design of gecko- and octopus-inspired adhesives is dominated by the geometry; thus, the diameter, length, density, and orientation of the individual components (fibrous pads and suction cups) need to be adjusted carefully [15]. To obtain optimized micropatterns on the polymer matrix, sophisticated and complicated photolithography and replica molding methods are required [16]. In this work, PDMS replicas with suction cup-like negative patterns were fabricated conveniently using vertically etched microholes, as shown in Fig. 1. The hardness or softness of the PDMS patches could be adjusted by the amount of the curing agent. The PDMS patches cured with a higher amount of curing agent (15%) had a Young's modulus of ~2.8 MPa of and relatively rigid properties, while PDMS with a lower amount of curing agent (5%) of (with a Young's modulus of ~0.8 MPa) was too soft [5]. Specifically, hard polymers store their elastic energy in their backbone instead of attaching to the surface, and soft polymers can be bent easily and adhere to each other instead of adhering to the surface [17]. Therefore, the balance between softness and hardness of PDMS is im-

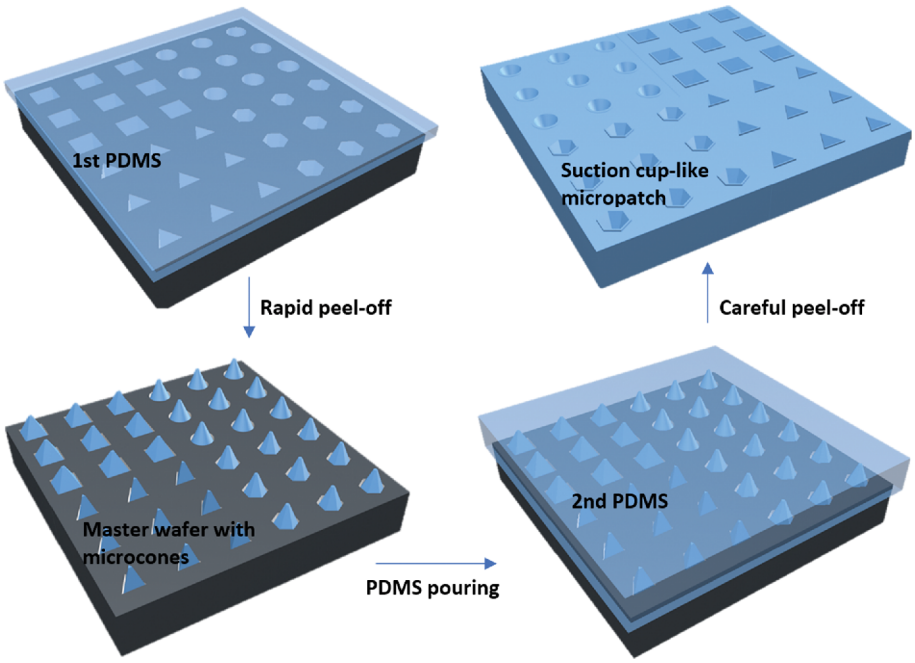

Fig. 1. Schematic illustration of the fabrication of octopus sucker-like positive pattern on the 1st PDMS and suction cup-like negative pattern on the 2nd PDMS as dry adhesive micropatches.

portant to their adhesiveness and elasticity as dry adhesives. In the fabrication of the first PDMS replica, 10% curing agent was used and thus a relatively hard PDMS patch was obtained. Then, the 10%-PDMS was rapidly peeled off from the master wafer to obtain inner microholes with microcone structure on the wafer. The positive cone structure formed a negative hole structure during fabrication of the second PDMS replica. Finally, suction cup-like micropatches were obtained. The second PDMS patch was cured using 7.5% curing agent to provide relative softness compared with the first PDMS patch. Kwak et al. also reported that the fraction of 7.5% exhibited the best adhesion performance [16]. To determine the softness of the PDMS, the adhesion energy between the AFM probe and the surface of the PDMS was measured using the force-distance curve, which was measured by AFM. The cantilever used in this case (PPP-CONTSCR, Park Systems) had a force constant of 0.2 N/m. The stickier and softer PDMS had stronger contact with the probe tip on the cantilever. The attraction forces of the probe tip on the 10%- and 7.5%-PDMSs were approximately 1.6 nN and 4.1 nN, respectively. Therefore, 7.5%-PDMS is softer compared with 10%-PDMS.

The surface morphologies of the PDMS replicas and the wafer were observed by AFM as shown in Figs. 2 and 3. The first PDMS replica formed a positive pattern from the master wafer and showed an octopus sucker-like shape (Fig. 2(a)). Deep microholes with depth of 12 μm in the master wafer were filled completely with 10%-PDMS. The deep reactive-ion etching (DRIE) process is a

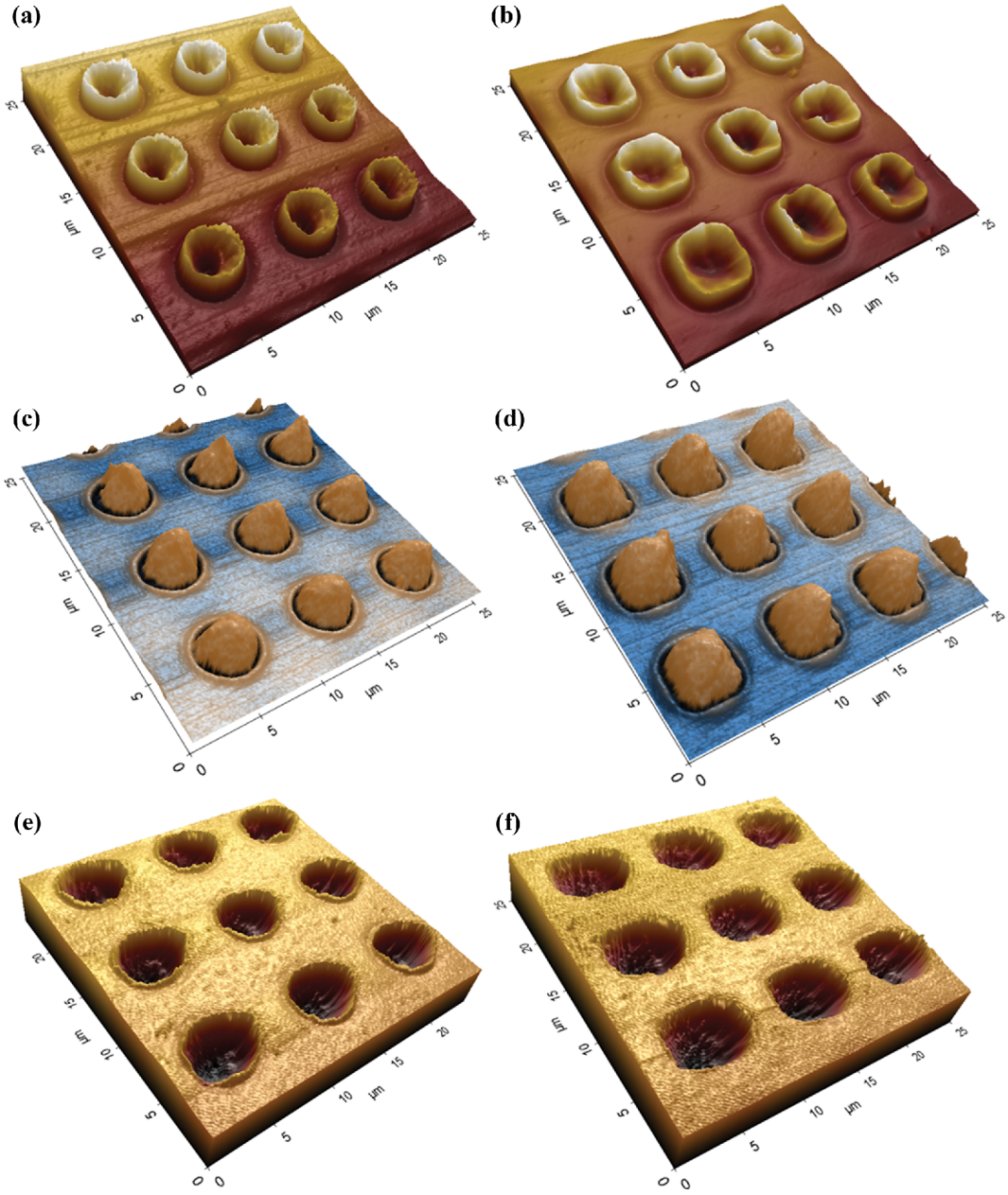

Fig. 2. AFM images of the 1st PDMS (a) and (b), the wafer with microcones (c) and (d), and the 2nd PDMS (e) and (f), which was fabricated by replica molding based on circular (a), (c), and (e) and square (b), (d), and (f) shaped patterns on the master wafer.

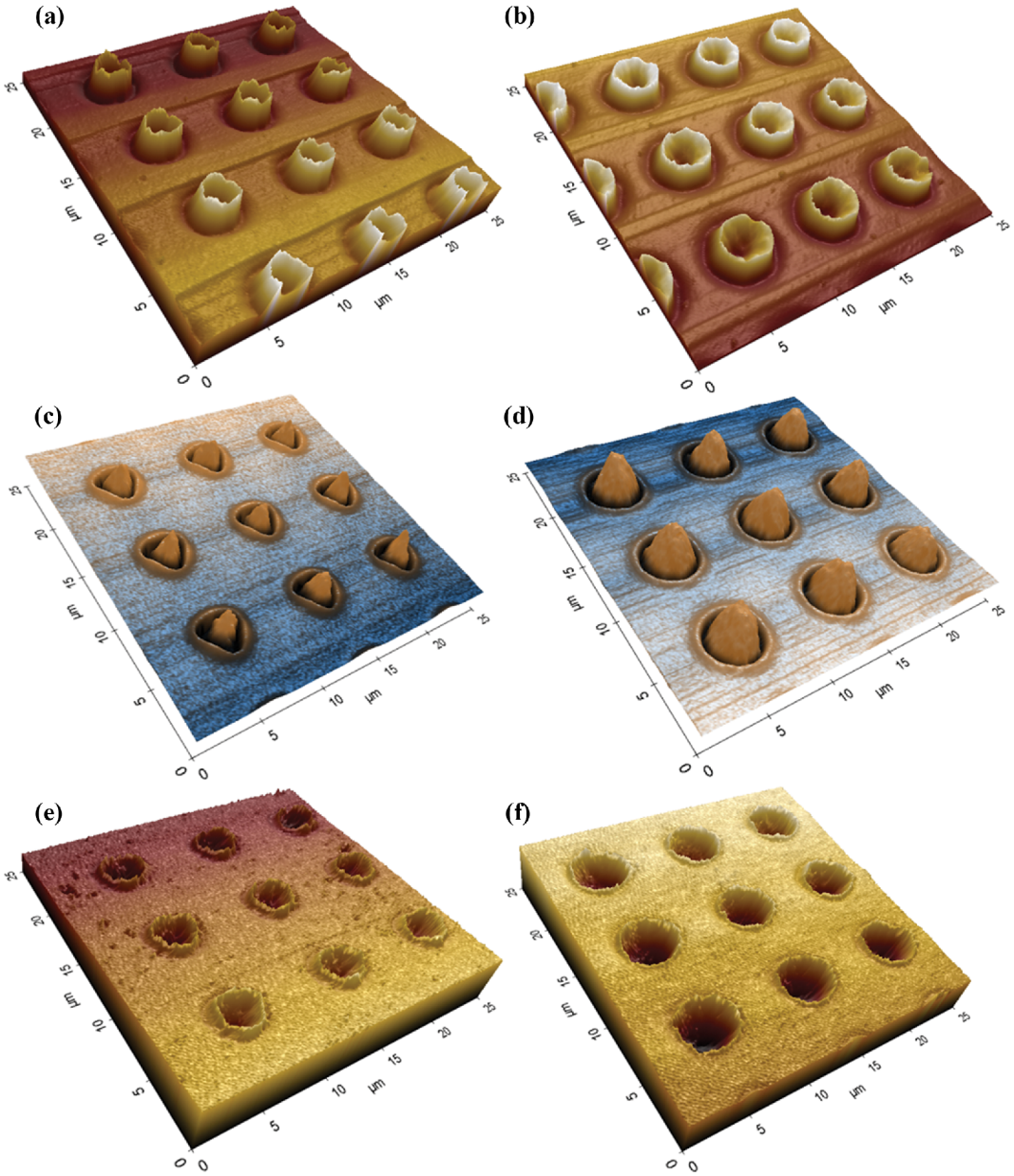

Fig. 3. AFM images of the 1st PDMS (a) and (b), the wafer with microcones (c) and (d), and the 2nd PDMS (e) and (f), which was fabricated by replica molding based on triangular (a), (c), and (e) and hexagonal (b), (d), and (f) shaped patterns on the master wafer.

time-multiplexed etching method that repeatedly alternates between SF_6 etching and passivation to achieve nearly vertical structures. These etching-passivation steps are repeated several times, resulting in an undulating sidewall of the microholes [18]. Therefore, a relatively hard PDMS was stuck on the wall of the microholes and could not be removed gently from the microhole when it was rapidly peeled off from the master wafer. Because the total pulling force was applied to the top of the micropillars stuck in microholes, the weakest part was torn out. All positive patterns of the first PDMS replica were separated from the master wafer and the residual PDMS formed a cone structure in the master wafer (Fig. 2(c)). Specifically, AFM images of the first PDMS replica showed a perfect inverse structure with respect to the used wafer. The as-prepared PDMS replica was similar to the reported octopus-inspired architecture [12,13,19]. The method of forming an octopus-like micropattern in this study was simple and fast compared with the fabrication of gecko-like dry adhesives, which require multiple complicated photolithography processes [8,20]. The second 7.5%-PDMS replicas were obtained from the used master wafer containing a microcone structure of 10%-PDMS. If the same amount of curing agent was used in the second molding step, the second PDMS was stuck to the first PDMS in wafer. The 7.5%-PDMS was softer compared with the 10%-PDMS; thus, it could be peeled off smoothly from the used wafer. As shown in Fig. 2(e), the second set of PDMS replicas showed a negative pattern with respect to the microholes, which resembled the suction cup. Finally, both positive octopus-

Table 1. Depth and width of microholes in 10%- and 7.5%-PDMS replicas, measured by AFM

Shape	10%-PDMS		7.5%-PDMS	
	Depth (mμ)	Width (μm)	Depth (μm)	Width (μm)
Triangle	0.395±0.039	2.724±0.156	0.541±0.025	3.043±0.105
Hexagon	0.444±0.032	3.527±0.065	0.752±0.058	4.082±0.074
Circle	0.529±0.018	3.965±0.031	0.929±0.040	4.956±0.215
Square	0.657±0.043	4.193±0.058	1.114±0.048	5.683±0.122

like and negative suction cup-like PDMS replicas could be conveniently obtained from a single master wafer. The morphology of PDMS replicas slightly varied with the shape (circle, square, triangle, and hexagon) of the master pattern. Table 1 shows detailed information on the depth and width of microholes in 10%- and 7.5%-PDMS replicas, and their cross-sectional profile is shown in Fig. 4. The depths of the patterns are listed in the order of shapes of triangle, hexagon, circle, and square. The depth and width of microholes in 7.5%-PDMS is deeper and wider than those of 10%-PDMS. Thus, the total adhesion force (F) induced by suction (F_n) and vdW forces (F_s) possibly depends on the morphology of the patterns in PDMS replicas.

In the adhesion mechanism of octopus suckers or suction cups, adhesion is generated by the sucker attaching to a target and inducing a negative pressure on the target surface material [21]. Octopus-inspired or suction cup-like adhesive systems require an ad-

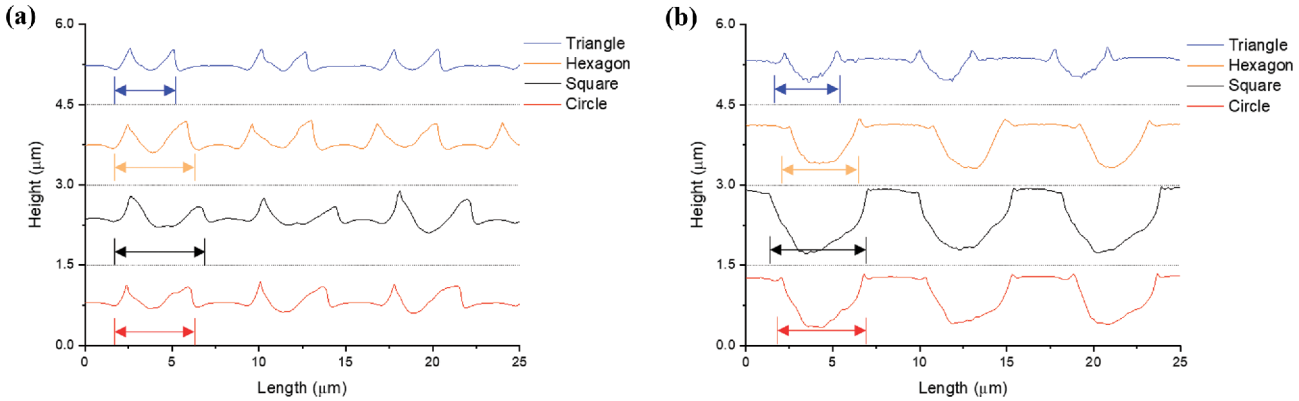

Fig. 4. Cross-sectional profiles of (a) positive and (b) negative patterns in the 10%-PDMS and 7.5%-PDMS replicas, respectively (The arrows represent the width of the unit pattern.).

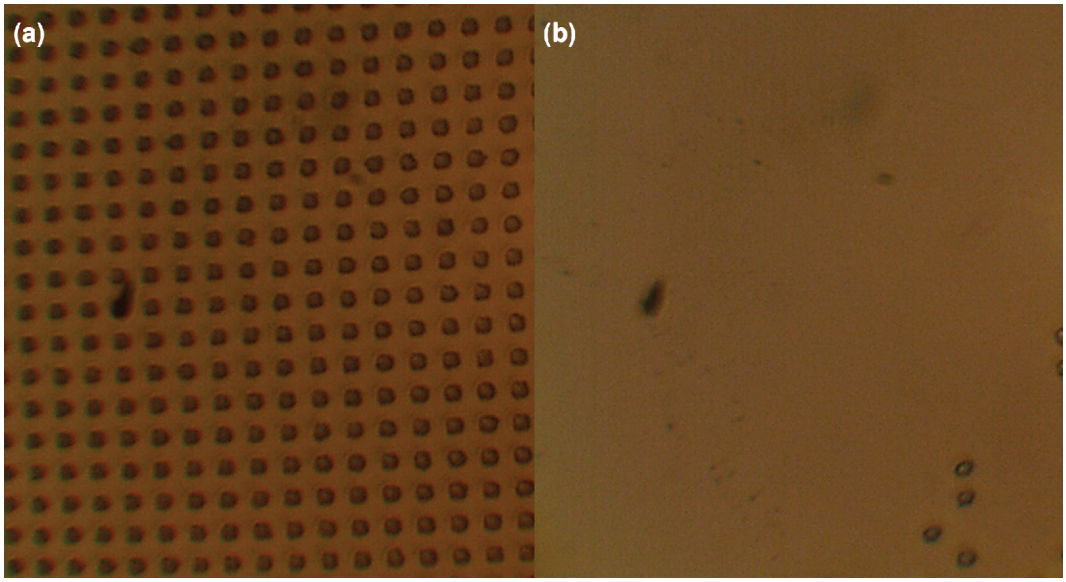

Fig. 5. Optical images of 7.5%-PDMS micropatch with square microholes attached on flat glass (a) before and (b) after the application of the preloading force to the film (the hole size is ~4 μm).

ditional suction force during the adhesive process to reduce the pressure inside the suction cups [19]. It is also our everyday experience that macroscopic suction cups require a preloading force to attach effectively to the surface [14]. Therefore, in our system, a preloading force (F_p) is also required for dry adhesion. The preloading force required to attach to the substrate can be observed directly using an optical microscope (HNM003, HiMax Tech). As shown in Fig. 5(a), the square pattern in the 7.5%-PDMS replica can clearly be observed before the application of the preloading force. After a preloading force of 2.4 N/cm^2 was applied on the substrate via compression with increasing weight, the suction cup-like microholes clearly disappeared (Fig. 5(b)). Note that the microholes were fully compressed and exerted negative pressure (ΔP) to realize the suction effect on the surface. Therefore, in the subsequent measurement of the total adhesion force of the as-prepared PDMS replicas, the preloading force was set to 2.444 and 2.693 N/cm^2 for 10%- and 7.5%-PDMS, respectively.

The suction force is mainly related to the effective area (A_h) of the suction cup and the compressing pressure (ΔP) [14,22]. To determine the total adhesion force of the PDMS replicas, the surface area (S_h) of the individual microholes in the first and second replicas needed to be calculated. High-resolution AFM images of each micropatterns could be obtained as shown in Fig. 6, and their surface area was calculated with a graphing and analysis software.

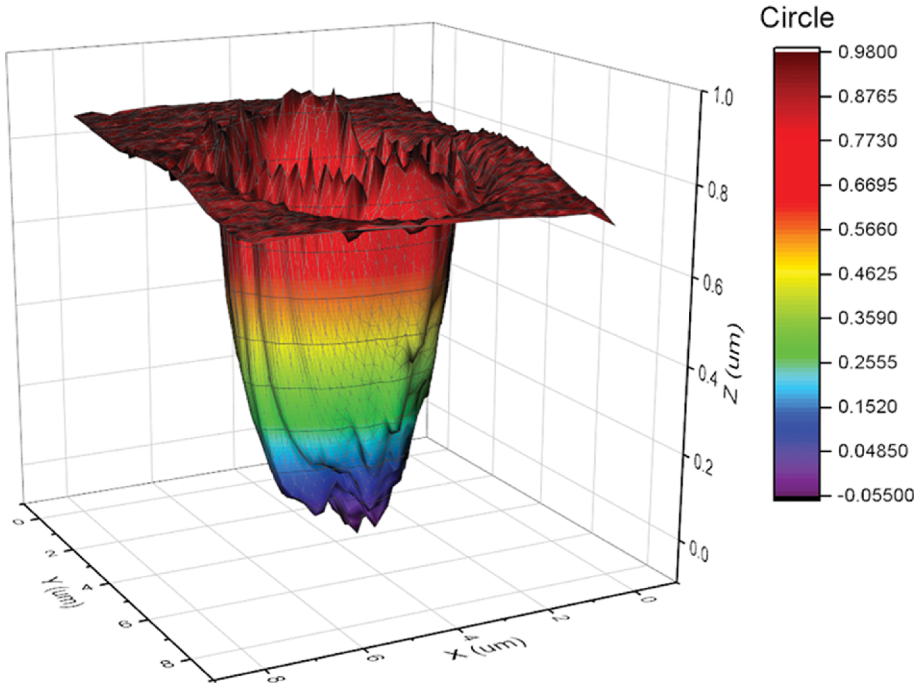

Fig. 6. High-resolution AFM image for the evaluation of the surface area of 7.5%-PDMS with circular microholes.

Table 2. Surface area and total adhesion force of 10%- and 7.5%-PDMS micropatches

Samples		Triangle	Hexagon	Circle	Square
10%-PDMS	A_h (cm^2)	0.093	0.157	0.206	0.232
	A_t (cm^2)	1.043	1.055	1.067	1.073
	F_p (N/cm^2)	2.444	2.444	2.444	2.444
	F_n (N/cm^2)	0.945	1.588	2.088	2.351
	F_s (N/cm^2)	4.612	4.665	4.718	4.745
	F_{tc} (N/cm^2)	8.001	8.697	9.250	9.540
	F_{te} (N/cm^2)	9.792±0.238	10.214±1.019	10.698±0.385	11.401±0.313
7.5%-PDMS	A_h (cm^2)	0.127	0.222	0.332	0.440
	A_t (cm^2)	1.147	1.181	1.210	1.421
	F_p (N/cm^2)	2.693	2.693	2.693	2.693
	F_n (N/cm^2)	1.287	2.258	3.367	4.458
	F_s (N/cm^2)	6.525	6.719	6.884	8.084
	F_{tc} (N/cm^2)	10.505	11.670	12.944	15.235
	F_{te} (N/cm^2)	13.082±0.900	14.798±0.937	15.763±0.601	15.996±1.137

The number (N) of microholes per unit area (1 cm^2) is 1,562,500, because the interdistance between the centers of the neighboring microholes is 8 μm. The total effective area for suction cups in the PDMS micropatches was obtained by multiplying the number and the area of microholes (A_h=NS_h). In this study, the total surface area (A_t) was also calculated with the same method to determine the shear force (F_s) on the contact area induced by vdW force. The total adhesion force (F_{tc}) can be calculated with F_p, F_n, and F_s, where, F_p is the force of compression pressure required to be applied for the initial adhesion, F_n (=$\Delta P_{max}A_h$) is the suction effect in the normal direction to the surface, and F_s (=F_vA_t) is the shear force by vdW attraction (F_v) between the parent PDMS and the substrate. The maximum negative pressure was assumed as 10.132 N/cm^2 to form full compression. The shear stress (F_v) of the parent PDMS without micropatterns was measured by a custom-made pulley arrangement at different loadings under same preloading force. The total adhesion forces of the parent 10%- and 7.5%-PDMSs were 6.866±1.436 and 8.382±1.030 N/cm^2, respectively; thus, their shear stresses were 4.422±1.394 and 5.689±1.003 N/cm^2, respectively. The theoretically calculated surface area and total adhesion force of the two PDMS replicas are summarized in Table 2. The ratio of F_n to F_s for 10%- and 7.5%-PDMS micropatches with square microholes is about 1.8 and 2.0 for both cases. While the adhesion force of gecko-inspired adhesives is due to only F_s induced by vdW attraction, octopus-inspired or suction cup-like adhesives have higher adhesion force due to the sum of F_n, F_s, and F_p as well. The calculated data shows that the square patterns of 7.5%-PDMS patch have larger adhesion force than that of 10%-PDMS patch, because the effective area of the microholes fabricated with square patterns is large compared with that of other shapes.

The total adhesion force of all samples was experimentally measured and shown in Table 2 and Fig. 7. Although the deviation between the calculated force (F_{tc}) and the experimentally measured force (F_{te}) is in the range of ~1.5-2.0 N/cm^2, the trends of the total adhesion force together with the shape of the micropatterns are in good agreement. In the literature, mushroom-like adhesives exhibited 2-8 N/cm^2 [3,8] and octopus-like adhesives had 4-12 N/cm^2 forces [13]. The total adhesion force of our samples is in the range of the reported adhesion force. In addition, to assess the repeatability of the measurement, the attachment/detachment of the as-prepared samples on the glass surface was performed for over 100 cycles. As shown in Fig. 8, the adhesion force of 10%- and 7.5%-PDMS micropatches with circular micropatterns is approximately maintained without dramatic degradations. Other patterns also showed similar features to that shown in Fig. 8. No structural collapses occurred after multiple attachments and detachments; therefore, the as-prepared micropatches fabricated in this study are suitable to be used as dry adhesives.

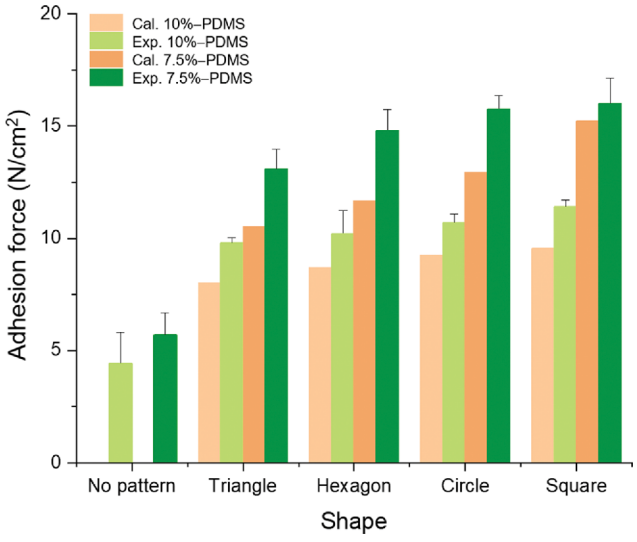

Fig. 7. Adhesion force of the as-prepared micropatches with four different shapes of positive and negative patterns on 10%- and 7.5%-PDMS.

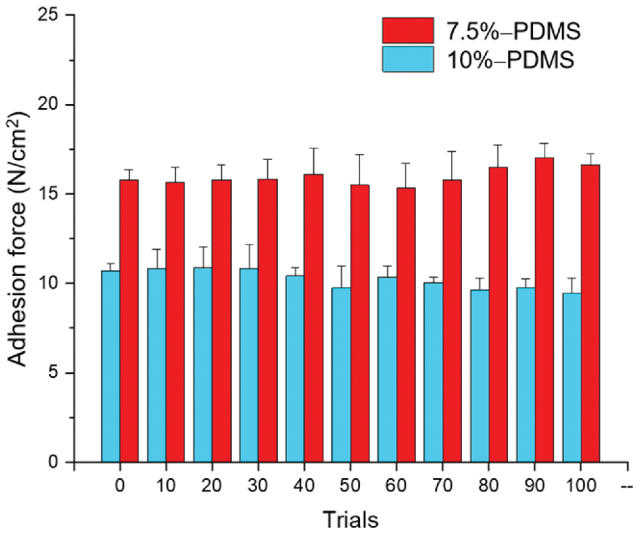

Fig. 8. Change in adhesion force for circular pattern on 10%- and 7.5%-PDMS during the repetitive attach/detach test of 100 cycles.

CONCLUSIONS

Octopus-like and suction cup-like micropatterns were successfully fabricated on PDMS patches by simple replica molding using a single master wafer with 12-μm -deep microholes. The fabrication method used in this study to form PDMS micropatches was simpler and faster than the fabrication of gecko-like dry adhesives. The softness of the positive and negative micropatterns was tested by measuring the force-distance curve in the AFM analysis, and it showed that the 7.5%-PDMS patch was softer than the 10%-PDMS one. As the suction cup-like adhesive systems require a preloading force during the adhesive process to reduce the pressure inside the suction cups, a fixed preloading force was applied to dry adhesives. The total adhesion force of microsuckers was induced both by the elasto-capillary effects on the suction forces and the dynamic contact effect on vdW forces; it was calculated by summing the preloading force (F_p), suction force (F_n), and shear force (F_s). The total force mainly depended on the effective area of micropatterns for both the 10%- and 7.5%-PDMS micropatches. When the adhe-

sion force was experimentally measured by a custom-made pulley system using increasing weight, the 7.5%-PDMS patch with square microholes showed a high adhesion force of ~16 N/cm^2. In addition, high repeatability of the attach/detach process of suction cup-like micropatches was maintained over a 100-times cycling test. In conclusion, the suction cup-like PDMS micropatches formed in our study have high potential in dry adhesives applications.

ACKNOWLEDGEMENTS

This work was supported by the National Research Foundation of Korea (NRF-2017R1A2B4001829).

REFERENCES

1. C. Creton, *MRS Bull.*, **28**, 434 (2003).
2. L. Qie and M. A. Dubé, *Inter. J. Adhes. Adhes.*, **30**, 654 (2010).
3. A. K. Singh, B. P. Panda, S. Mohanty, S. K. Nayak and M. K. Gupta, *Korean J. Chem. Eng.*, **34**, 3028 (2017).
4. H. E. Jeong and K. Y. Suh, *Nano Today*, **4**, 335 (2009).
5. W. G. Bae, D. Kim, M. K. Kwak, L. Ha, S. M. Kang and K. Y. Suh, *Adv. Healthcare Mater.*, **2**, 109 (2013).
6. K. Jin, Y. Tian, J. S. Erickson, J. Puthoff, K. Autumn and N. S. Pesika, *Langmuir*, **28**, 5737 (2012).
7. H. E. Jeong, M. K. Kwak and K. Y. Suh, *Langmuir*, **26**, 2223 (2010).
8. Y. Wang, H. Hu, J. Shao and Y. Ding, *ACS Appl. Mater. Interfaces*, **6**, 2213 (2014).
9. D. Brodoceanu, C. T. Nauer, E. Kroner, E. Arzt and T. Kraus, *Bioinspir. Biomim.*, **11**, 051001 (2016).
10. M. Follador, F. Tramacere and B. Mazzolai, *Bioinspir. Biomim.*, **9**, 046002 (2014).
11. H. Yi, I. Hwang, M. Sung, D. Lee, J.-H. Kim, S. M. Kang, W.-G. Bae and H. E. Jeong, *Int. J. Precis. Eng. Manuf.*, **1**, 347 (2014).
12. S. Baik, D. W. Kim, Y. Park, T.-J. Lee, S. H. Bhang and C. Pang, *Nature*, **546**, 396 (2017).
13. S. Baik, J. Kim, H. J. Lee, T. H. Lee and C. Pang, *Adv. Sci.*, **5**, 1800100 (2018).
14. S. Qiao, L. Wang, K.-H. Ha and N. Lu, *Soft Matter*, **14**, 8509 (2018).
15. A. del Campo and E. Arzt, *Macromol. Biosci.*, **7**, 118 (2007).
16. M. K. Kwak, H.-E. Jeong and K. Y. Suh, *Adv. Mater.*, **23**, 3949 (2011).
17. R. Spolenak, S. Gorb and E. Arzt, *Acta Biomater.*, **1**, 5 (2005).
18. M. T. Ghoneim and M. M. Husain, *Small*, **13**(16), 1601801 (2017).
19. Y.-C. Chen and H. Yang, *ACS Nano*, **11**, 5332 (2017).
20. M. K. Kwak, H. E. Jeong, W. G. Bae, H.-S. Jung and K. Y. Suh, *Small*, **7**, 2296 (2011).
21. F. Tramacere, N. M. Pugno, M. J. Kuba and B. Mazzolai, *Interface Focus*, **5**, 20140050 (2014).
22. J. Zou, J. Wang and C. Ji, *Sci. Rep.*, **6**, 37221 (2016).